Tetragonally Packed Cylinder Structure of Comb−Coil Block Copolymer Bearing Heteroarm Star Architecture

Wei-Shan Chiang,[†] Chia-Hung Lin,[‡] Chao-Lin Yeh,[†] Bhanu Nandan,[†,⊥] Pei-Nan Hsu,[†] Chiu-Wei Lin,[†] Hsin-Lung Chen,*[,†] and Wen-Chang Chen*[,‡,§]

Department of Chemical Engineering, National Tsing Hua University, Hsin-Chu 30013, Taiwan; Department of Chemical Engineering, National Taiwan University, Taipei 10617, Taiwan; and Institute of Polymer Science and Engineering, National Taiwan University, Taipei 10617, Taiwan

Received October 23, 2008
Revised Manuscript Received January 6, 2009

Introduction

Block copolymers form a special class of soft materials capable of self-assembling into a variety of long-range ordered nanostructures.[1] In the melt state the microphase separation between the incompatible blocks generates the micelle comprising the microdomain composing of the minority block and the corona consisting of the majority block. The classical microdomains are lamellae, cylinder, and sphere. The interaction between the micelles further results in long-range ordered spatial arrangement of the microdomains.

The cylindrical domains formed by diblock copolymers have been found to organize almost exclusively in a hexagonal lattice due to its efficiency for space filling. Tetragonal lattice is another type of packing symmetry which is rarely observed unless some special factors are introduced to modify the intermicellar interaction. The introduction of liquid crystallinity into the majority block is an approach to induce tetragonal packing of the cylindrical microdomains formed by the other amorphous block.[2−4] For instance, the polystyrene (PS) cylinders in a diblock copolymer, polystyrene-*block*-poly(2-(3-cholesteryloxycarbonyloxy)ethyl methacrylate) (PS-*b*-PChEMA), in which the PChEMA block was liquid crystalline, were found to organize into a tetragonal lattice.[2] In fact, tetragonal phase in the past has been observed in some other liquid crystalline systems such as complexes of cationic dendronized polymers with anionic lipids with the polymer backbone representing the cylinder,[5,6] ionic liquid crystal denrimers,[7,8] rod−coil multiblock liquid crystalline oligomers with the rods forming the cylinders,[9] and DNA/dendrimer complexes with the DNA rods organizing into tetragonal lattice for effective charge matching.[10,11] The characteristic lengths of the nanostructures in these systems are of several nanometers. Tetragonal lattices with the length scale of several tens of nanometers have been observed for linear and heteroarm ABC triblock copolymers composed of two types of cylinders formed by two of the block chains.[12,13] Recently, inspired by the work on ABC triblock copolymer, tetragonal arrangement of cylinders was also shown in blends of diblock copolymers.[14]

Previously, we have demonstrated that the mesomorphic order associated with the comb block in a linear comb−coil diblock copolymer was able to induce the tetragonally packed cylinder structure.[4] This comb−coil diblock was formed by the selective complexation of the poly(4-vinylpyridine) (P4VP) block in a linear PS-*b*-P4VP with the surfactant dodecylbenzenesulfonic acid (DBSA). The copolymer self-assembled into the cylinder-within-lamellae structure,[15] in which the PS cylinders were embedded in the matrix composing of the lamellar mesophase organized by the comb block. The cylindrical microdomains were found to pack in the typical hexagonal lattice when the overall grafting density of the comb block approached the stoichiometric value; however, tetragonal packing became the stable structure at the intermediate binding fraction of DBSA to P4VP block.[4] The packing symmetry was further found to be governed by the orientation of the smaller scale lamellae with respect to the larger scale PS cylinders. The hexagonal lattice was favored when the two entities showed the "orthogonal orientation", where the smaller scale lamellae stacked along the cylinder axis; on the other hand, the "edge-on arrangement" of the smaller scale lamellae, where the side chains of the comb blocks lay flatly on the plane of the cylinder cross section, induced tetragonal packing of the cylinders.

Our other studies of comb−coil block copolymers[16−18] have revealed that the molecular architecture could affect their self-organization behavior in terms of the domain spacing and the relevant order−disorder transition temperatures. For instance, the order−disorder transition temperatures associated with the structures at both length scales increased significantly in the heteroarm star comb−coil copolymers compared with their linear counterparts.[17,18] In this study, we are interested in exploring if the unusual tetragonally packed cylinder structure is also accessible for the comb−coil copolymer bearing heteroarm star architecture. Here we prepare the heteroarm comb−coil copolymer by selective complexation of DBSA with the P4VP block in a PS_n−$P4VP_n$ heteroarm star copolymer. It will be shown that the PS cylindrical domains in the copolymer with stoichiometric surfactant binding in the comb block display hexagonal packing, while those in the system with the overall binding fraction of 0.4 organize into a tetragonal lattice. The difference in packing symmetry is also found to stem from the different relative orientation of the two structural entities with different length scales.

Experimental Section

The heteroarm star PS_n−$P4VP_n$, with the average arm number n of both PS and P4VP blocks being 2.6, was prepared by a three-step sequential copolymerization.[17] The number-average molecular weights of PS and P4VP blocks were both 8800, and the polydispersity index of the copolymer was 1.27.

The complexes of the copolymer with DBSA (Acros, mixture of C10−C13 isomers) were prepared according to the procedure described previously.[4] The overall binding fraction of DBSA on P4VP block is denoted by x, which expresses the average number of DBSA molecules bound with a 4VP monomer unit prescribed by the feed ratio of DBSA and P4VP block in the copolymer. The comb−coil copolymers with $x = 0.4$ and 1.0 were prepared here, as they both displayed cylinder-within-lamellae morphology. The corresponding volume fraction of PS block (f_{PS}) is 0.31 and 0.19, respectively.

* To whom correspondence should be addressed. E-mail: hlchen@che.nthu.edu.tw (H.-L.C); chenwc@ntu.edu.tw (W.-C.C.).
† National Tsing Hua University.
‡ Department of Chemical Engineering, National Taiwan University.
§ Institute of Polymer Science and Engineering, National Taiwan University.
⊥ Present address: Leibniz Institute of Polymer Research Dresden, Hohe Strasse 6, 01069 Dresden, Germany.

10.1021/ma802386s CCC: $40.75
Published on Web 02/23/2009

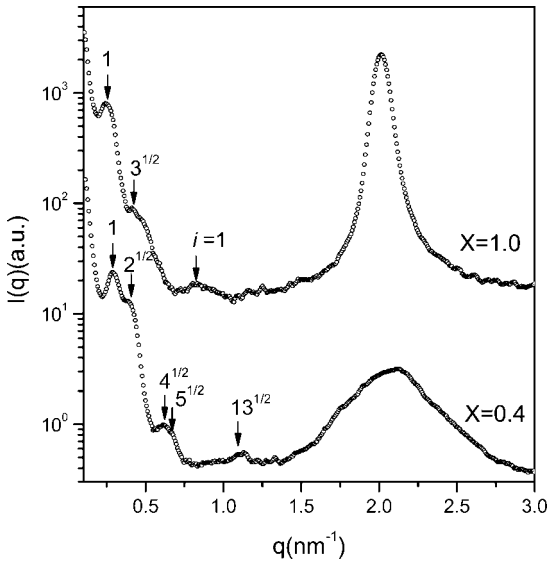

Figure 1. SAXS profiles of the two PS−P4VP(DBSA) heteroarm star comb−coil copolymers under study. The overall binding fractions (x) of DBSA on P4VP(DBSA) comb blocks are 1.0 (stoichiometric binding) and 0.4. The relative positions of the lattice peaks are marked by the arrows. The PS cylindrical microdmains are found to pack in the hexagonal and tetragonal lattice in the copolymers with $x = 1.0$ and 0.4, respectively.

Small-angle X-ray scattering (SAXS) measurements were performed using a Bruker Nanostar SAXS instrument equipped with a two-dimensional position-sensitive detector (Bruker AXS) with 512 × 512 channels. The real-space morphology of the comb−coil copolymers was observed by a JEM-2000EX II transmission electron microscope operated at 100 kV. The film specimens were microtomed at −50 °C using a Reichert Ultracut E low-temperature sectioning system.

Results and Discussion

Here we have prepared the heteroarm star comb−coil copolymers with the overall binding fraction of the comb blocks of 1.0 (i.e., the stoichiometric binding) and 0.4. Figure 1 displays the SAXS profiles of the two copolymers. For the system with $x = 1.0$, the SAXS peaks in the low-q region ($q < 1.5$ nm^{-1}) are associated with the larger scale copolymer domain structure arising from the microphase separation between PS and P4VP(DBSA) comb blocks.[4] The peak situating at 2.0 nm^{-1} arises from the smaller scale structure organized by the comb block, where the microphase separation between the P4VP backbone and DBSA side chains yields a lamellar structure with the interlamellar distance of 3.1 nm.[4] The low-q SAXS peaks display the position ratio of $1:3^{1/2}:4^{1/2}$, signaling the formation of hexagonally packed PS cylinders[19] with the interdomain spacing (D) of 28.9 nm calculated from the primary peak position (q_m) via $D = (4/3)^{1/2}2\pi/q_m$. The experimentally observed scattering profile can be fitted by the paracrystalline model of hexagonally packed cylinders considering the polydispersities of the cylinder radius and length, the domain (grain) size of the lattice, and the lattice distortion by thermal fluctuations (see Supporting Information).[19]

The copolymer with $x = 0.4$ is seen to exhibit a different scattering pattern. The high-q peak situating at 2.1 nm^{-1} becomes broader, signaling a poorer order of the smaller scale lamellae. It should be noted that the large breadth of this peak does not mean that it is the correlation hole peak arising from the characteristic concentration fluctuations of the comb blocks in the disordered state, since the intensity in its tail region exhibits the q^{-4} dependence. This corresponds to the scattering

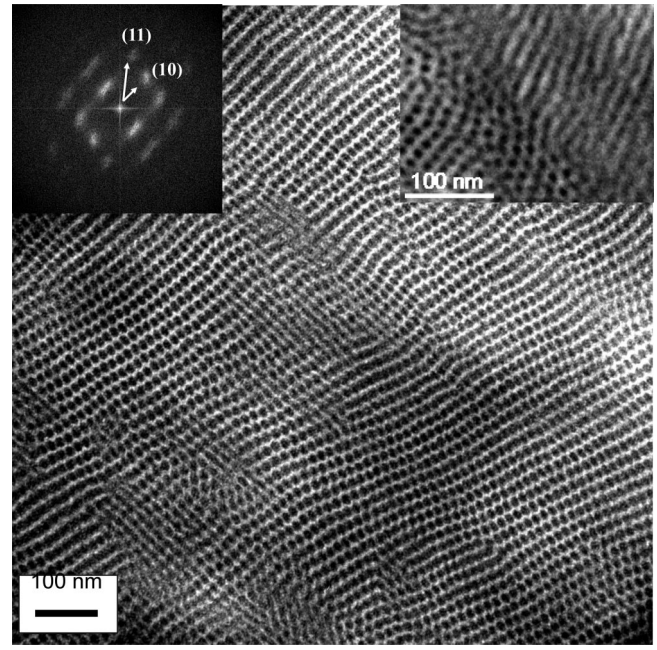

Figure 2. TEM micrograph showing the cross-sectional view of the PS cylinders in the PS−P4VP(DBSA) heteroarm star comb−coil copolymer with $x = 0.4$. The upper right inset shows the coexistence of the images of striation and circles/ellipsoids corresponding to the side view and the top view of PS cylinders, respectively. The upper left inset displays the Fourier-transform pattern of the real-space image. The PS cylinders are seen to pack in a tetragonal lattice.

from a two-phase system with sharp phase boundary prescribed by the Porod's law.[20] Moreover, the formation of the lamellar mesophase by the P4VP(DBSA) comb block was also evidenced by the mesomorphic birefringent pattern observable under polarized optical microscopy.

In the low-q region, a peak situating at ca. 0.4 nm^{-1} is observed as a shoulder of the primary peak. The positions of the observed scattering peaks now follow the ratio of $1:2^{1/2}:4^{1/2}:5^{1/2}:13^{1/2}$, which is in accord with that displayed by the previously studied linear PS-*b*-P4VP(DBSA) with $x = 0.5$ and 0.6 showing tetragonally packed cylinder structure.[4] In this case, the $2^{1/2}$, $4^{1/2}$, $5^{1/2}$, and $13^{1/2}$ peaks are associated with the (11), (20), (21), and (32) diffraction planes, respectively, of a square lattice organized by the PS cylindrical microdomains.[19] The observed peak positions agree reasonably well with those prescribed by the paracrystalline model of square-packed cylinders (see Supporting Information). The absence of other characteristic peaks such as (22), (30), and (31) may be due to the small grain size, lattice distortion, and the intervention of the form factor of PS cylinders. The large breadth of the peak associated with the smaller scale structure of the comb block, which extends to the intermediate q region, may also mask these higher order peaks.

The tetragonal packing of the PS cylinders in the system with $x = 0.4$ is further confirmed by the real-space morphological observation by TEM. Figure 2 shows the TEM micrograph of the ultrathin section stained by RuO_4. Since RuO_4 is a preferential staining agent for PS, the PS cylindrical domains would appear dark in the micrograph. The upper right inset of the figure shows the coexistence of the images of striation and dark circles/ellipsoids corresponding to the side view and the top view of cylinders, respectively, which confirms that the PS domains are indeed cylinder in shape. The tetragonal organization can be demonstrated clearly from the cross-section image of the PS cylinders in the main body of the micrograph, which

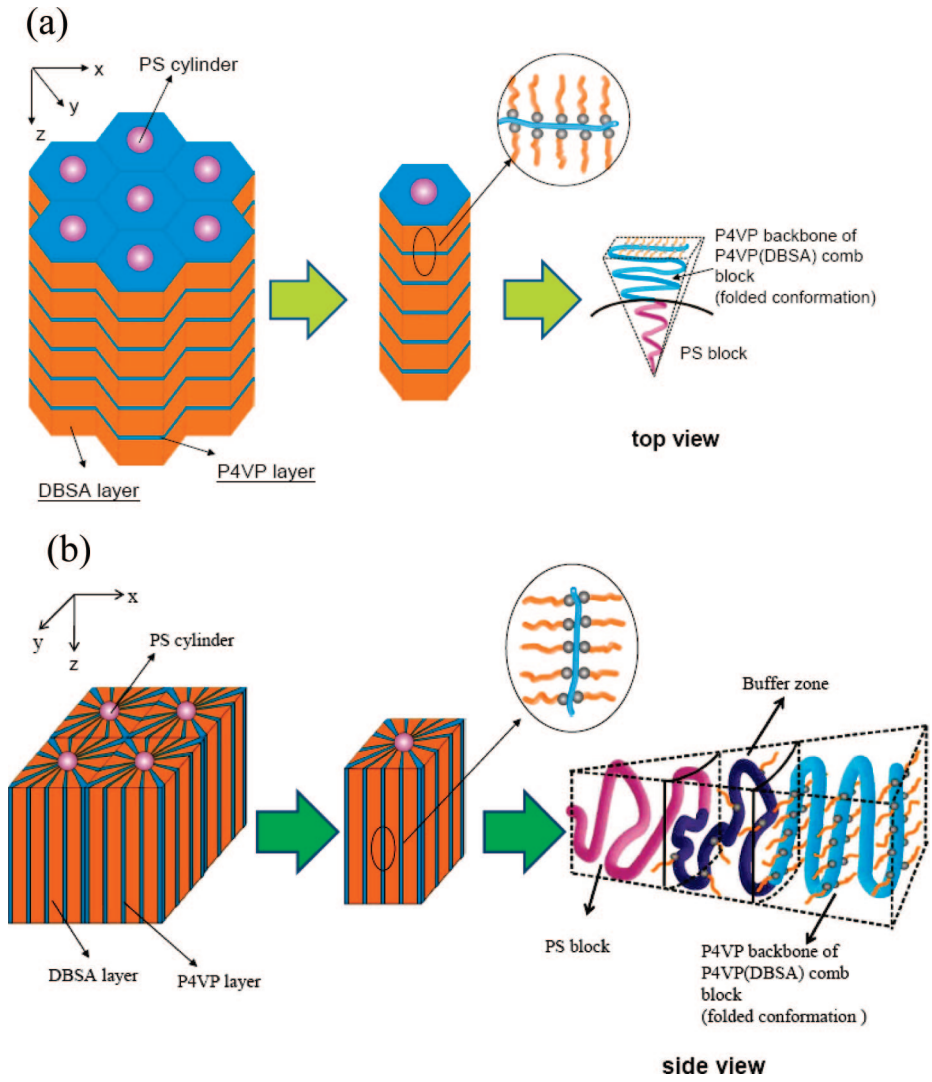

Figure 3. Schematic illustrations of the organization of the PS cylinders and the smaller scale lamellae formed by P4VP(DBSA) comb blocks in the system showing (a) hexagonally packed cylinder structure and (b) tetragonally packed cylinder structure. For the clarity of presentation, only one PS block and one P4VP block attaching to a junction point are drawn. The smaller scale lamellae displays the orthogonal orientation in the hexagonal structure in (a), where the lamellae stack along the cylinder long axis. For the tetragonal structure in (b), the smaller scale lamellae adopt the edge-on arrangement, where the side chains of the comb blocks tend to lie flatly on the plane of the cylinder cross section (i.e., *xy*-plane). In both cases, the P4VP backbone of the comb block should adopt some folded conformations to allow PS block to relax.

yields the 4-fold symmetry in the corresponding Fourier-transform pattern (cf. the upper left inset).

Both the SAXS and TEM results have revealed that the heteroarm PS−P4VP(DBSA) comb−coil copolymer exhibits the same self-assembly behavior as its linear counterpart in terms of the effect of the overall binding fraction of comb block on the packing symmetry of the PS cylinders. For the system with stoichiometric binding the cylindrical domains pack into a hexagonal lattice whereas for the intermediate binding fraction (i.e., $x = 0.4$) the cylinders arrange in a tetragonal lattice. Using the linear PS-*b*-P4VP(DBSA) with large-scale alignment of the microdomains, we have demonstrated previously that the systems with high and intermediate binding fractions showed different orientation of the smaller scale lamellae with respect to the larger scale PS cylinder, and such a difference led to contrasting packing lattices of the cylindrical domains.[4] Two types of relative orientation were identified in the previous study, namely, the orthogonal orientation and the edge-on arrangement of the smaller-scale lamellae, as schematically illustrated in Figure 3. These orientations can be distinguished from the SAXS 2-D pattern obtained with the incident X-ray traveling perpendicular to the cylinder axis (called the "edge-view pattern"). For the orthogonal orientation, the smaller scale lamellae stack along the long axis of the cylinder (i.e., *z*-axis); in this case, the side chains of the comb blocks tend to align along the *z*-axis, such that the lamellar interface lies perpendicularly to the cylinder axis, as shown in Figure 3a. The corresponding edge-view SAXS pattern contains a pair of inner arcs associated with the (10) plane of the cylinder lattice at the equator and another pair of outer arc due to the (001) diffraction of the smaller scale lamellae at the meridian, or vice versa. For the edge-on arrangement of the smaller-scale lamellae, the side chains of the comb blocks tend to lie flatly on the plane of the cylinder cross section (i.e., the *xy*-plane), as schematically illustrated in Figure 3b. In the edge view, the normals to the interfaces of the lamellae attached to the lateral sides of the cylinders orient relatively perpendicular to the *z*-axis and hence results in two outer arcs located at the same direction as the inner arcs in the corresponding edge-view pattern. It was found previously that the PS cylinders packed in a hexagonal lattice when the two structural entities exhibited the "orthogonal orientation", while the edge-on arrangement of the smaller-scale lamellae induced tetragonal packing.[4]

Figure 4 shows the edge-view SAXS patterns of the two heteroarm star copolymers after subjecting to the large-amplitude

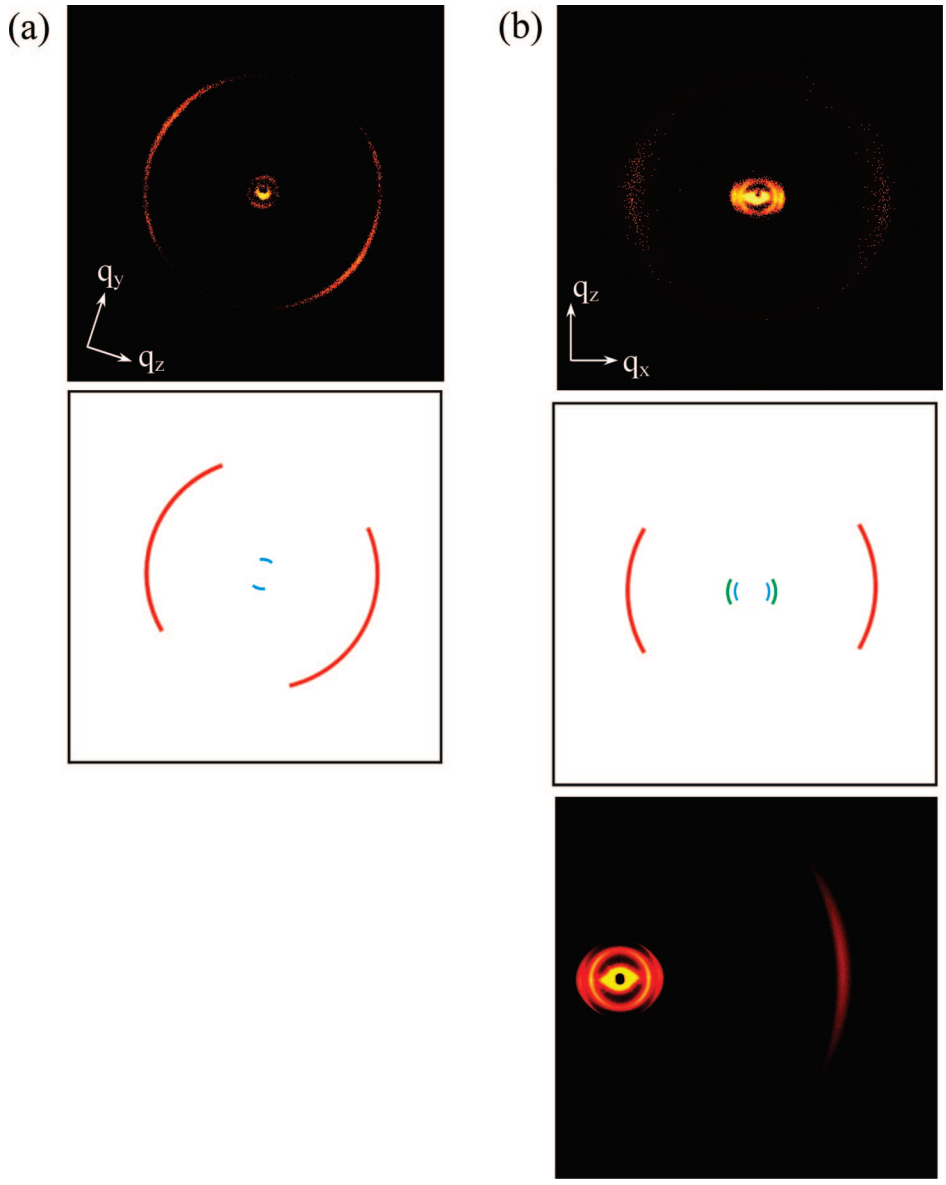

Figure 4. 2-D SAXS edge-view patterns of the shear-aligned PS−P4VP(DBSA) heteroarm star comb−coil copolymer with (a) $x = 1.0$ and (b) $x = 0.4$ for identifying the orientation of the smaller scale lamellae with respect to the long axis of PS cylinder. An additional pattern taken with the synchrotron radiation (conducted at the National Synchrotron Radiation Research Center, Taiwan) is shown for the system with $x = 0.4$ at the bottom of (b) due to the relatively weak intensity of the outer arc in the pattern collected with the in-house SAXS instrument. For the system with $x = 1.0$, the locations of the two pairs of arcs are perpendicular to each other, signaling that the two structural entities adopt the orthogonal orientation. For the copolymer with $x = 0.4$, the two pairs of arcs are both located at the equator, showing that the smaller scale lamellae adopt the edge-on arrangement.

oscillating shear treatment. For the system with $x = 1.0$ where the PS cylinders packed in hexagonal lattice, the locations of the two pairs of arcs are perpendicular to each other (Figure 4a), signaling that the two structural entities adopt the orthogonal orientation as that found for its linear counterpart. On the other hand, the arcs associated with the PS cylinders and the P4VP(DBSA) lamellae are both located at the equator for the copolymer with $x = 0.4$. This means that the smaller scale lamellae show the edge-on arrangement, which is again in parallel with that found in the linear system showing tetragonal lattice. Consequently, the present heteroarm star comb−coil copolymer with cylinder-within-lamellae morphology displays the same self-organization behavior as its linear counterpart in terms of the packing symmetry and corresponding relative orientation of the two structural entities.

It is not clear at the current stage why the smaller scale lamellae formed by the comb block with intermediate overall binding fraction would adopt the edge-on arrangement and how such a structure would result in the anomalous tetragonal packing of the PS cylinders. It is understandable why the P4VP(DBSA) comb block with stoichiometric binding tends to have the side chains aligning along the cylinder axis (i.e., to adopt the orthogonal orientation for the system), since the side chains near the cylinder interface would have been overly crowded if the comb blocks lay flatly on the *xy*-plane. Such a crowding effect is even more pronounced in the heteroarm star system as there are more than two block chains emanating from a given junction point at the cylinder interface.

In the case of intermediate overall binding fraction, the crowding of the side chains near the cylinder interface (if the side chains on the comb blocks are to lie flatly on the *xy*-plane) may be alleviated once the binding of DBSA to P4VP block is rather segregated. Here the P4VP subchains locating in the vicinity of the interface might only have a small degree of binding with DBSA, thereby creating a buffer zone. Considering the additional chain crowding arising from the attachment of

more than two block chains to a given junction point, this buffer zone is expected to be thicker in the heteroarm star system.

It should be noted that the observed interdomain distances of the cylindrical microdomains (= 28.9 and 21.6 nm for hexagonal and tetragonal lattice, respectively) are apparently smaller than 2 times the fully extended length of P4VP block in the present copolymer system ($\sim 2 \times 21 = 42$ nm). This means that the P4VP backbone in the comb block does not fully stretch normal to the interface of PS cylinder on forming the lamellar structure. In fact, if the P4VP block were fully extended, its corresponding covalently linked PS block would have been compressed considerably along the length direction in the tetragonal lattice and around the tangential direction in the hexagonal lattice of the cylinders. The entropic loss associated with such a compression can be alleviated if the P4VP backbone forming the P4VP lamellae in the smaller scale structure adopts some folded conformation,[21] as illustrated in Figure 3. The chain folding shortens the interdomain distance and effectively increases the cross-sectional area per junction point to allow the PS blocks to relax.

Conclusion

In summary, the anomalous tetragonally packed cylinder structure was also observed in the comb−coil PS−P4VP(DBSA) copolymer bearing heteroarm star architecture. Tetragonal lattice appeared at the intermediate binding fraction of DBSA on P4VP block, where the smaller scale lamellae adopted the edge-on arrangement with respect to the cylinder axis. The hexagonal packing became stable at the stoichiometric binding that resulted in the orthogonal orientation of the smaller scale lamellae with respect to the PS cylinder. The present result along with the previous one for the linear systems has thus demonstrated that the self-organization behavior in terms of the packing symmetry and the relative orientation of the two structural entities is essentially independent of the molecular architecture for the comb−coil copolymers.

Acknowledgment. We thank the financial support from the National Science Council under Contract NSC 97-2221-E-007-034-MY.

Supporting Information Available: Analysis of the SAXS profiles of the heteroarm PS−P4VP(DBSA) comb−coil copolymers with $x = 1.0$ and 0.4. This material is available free of charge via the Internet at http://pubs.acs.org.

References and Notes

(1) Hamley, I. W. *The Physics of Block Copolymers*; Oxford University Press: Oxford, 1998.
(2) Fischer, H. *Polymer* **1994**, *35*, 3786.
(3) Tenneti, K. K.; Chen, X.; Li, C. Y.; Tu, Y.; Wan, X.; Zhou, Q.-F.; Sics, I.; Hsiao, B. S. *J. Am. Chem. Soc.* **2005**, *127*, 15481.
(4) Chen, H. L.; Lu, J. S.; Yu, C. H.; Yeh, C. L.; Jeng, U. S.; Chen, W. C. *Macromolecules* **2007**, *40*, 3271.
(5) Canilho, N.; Kasëmi, E.; Schlüter, A. D.; Mezzenga, R. *Macromolecules* **2007**, *40*, 2822.
(6) Canilho, N.; Kasëmi, E.; Schlüter, A. D.; Ruokolainen, J.; Mezzenga, R. *Macromolecules* **2007**, *40*, 7609.
(7) Martin-Rapun, R.; Marcos, M.; Omenat, A.; Barbera, J.; Romero, P.; Serrano, J. L. *J. Am. Chem. Soc.* **2005**, *127*, 7397.
(8) Marcos, M.; Martin-Rapun, R.; Omenat, A.; Barbera, J.; Romero, P.; Serrano, J. L. *Chem. Mater.* **2006**, *18*, 1206.
(9) Lee, M.; Cho, B.-K.; Oh, N.-K.; Zin, W.-C. *Macromolecules* **2001**, *34*, 1987.
(10) Evans, H. M.; Ahmad, A.; Ewert, K.; Pfohl, T.; Martin-Herranz, A.; Bruinsma, R. F.; Safinya, C. R. *Phys. Rev. Lett.* **2003**, *91*, 75501.
(11) Liu, Y.-C.; Chen, H.-L.; Su, C.-J.; Lin, H.-K.; Liu, W.-L.; Jeng, U.-S. *Macromolecules* **2005**, *38*, 9434.
(12) Mogi, Y.; Nomura, M.; Kotsuji, H.; Ohnishi, K.; Matsushita, Y.; Noda, I. *Macromolecules* **1994**, *27*, 6755.
(13) Hückstädt, H.; Göpfert, A.; Abetz, V. *Macromol. Chem. Phys.* **2000**, *201*, 296.
(14) Tang, C.; Lennon, E. M.; Fredrickson, G. H.; Kramer, E. J.; Hawker, C. J. *Science* **2008**, *322*, 429.
(15) Ruokolainen, J.; ten Brinke, G.; Ikkala, O. *Adv. Mater.* **1999**, *11*, 777. Ruotsalainen, T.; Torkkeli, M.; Serimaa, R.; Makela, T.; Maki-Ontto, R.; Ruokolainen, J.; ten Brinke, G.; Ikkala, O. *Macromolecules* **2003**, *36*, 9437. Valkama, S.; Ruotsalainen, T.; Nykanen, A.; Laiho, A.; Kosonen, H.; ten Brinke, G.; Ikkala, O.; Ruokolainen, J. *Macromolecules* **2006**, *39*, 9327. Ruotsalainen, T.; Turku, J.; Hiekkataipale, P.; Vainio, U.; Serimaa, R.; ten Brinke, G.; Harlin, A.; Ruokolainen, J.; Ikkala, O. *Soft Matter* **2007**, *3*, 978.
(16) Nandan, B.; Lee, C. H.; Chen, H. L.; Chen, W. C. *Macromolecules* **2005**, *38*, 10117.
(17) Nandan, B.; Lee, C. H.; Chen, H. L.; Chen, W. C. *Macromolecules* **2006**, *39*, 4460.
(18) Chang, W. S.; Lin, C. H.; Nandan, B.; Yeh, C. L.; Rahman, M. H.; Chen, W. C.; Chen, H. L. *Macromolecules* **2008**, *41*, 8138.
(19) Förster, S.; Timmann, A.; Konrad, M.; Schellbach, C.; Meyer, A.; Funari, S. S.; Mulvaney, P.; Knott, R. *J. Phys. Chem. B* **2005**, *109*, 1347.
(20) Porod, G. *Kolloid-Z.* **1951**, *124*, 83. Porod, G. *Kolloid-Z.* **1952**, *125*, 51.
(21) Tsao, C.-S.; Chen, H.-L. *Macromolecules* **2004**, *37*, 8984.

MA802386S